Heliyon 10 (2024) e28912

Contents lists available at ScienceDirect

Heliyon

journal homepage: www.cell.com/heliyon

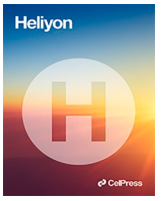

Research article

Bio inspired heuristic computing scheme for the human liver nonlinear model

Zulqurnain Sabir [a], Salem Ben Said [b,*], Qasem Al-Mdallal [b]

[a] Department of Computer Science and Mathematics, Lebanese American University, Beirut, Lebanon
[b] Department of Mathematical Sciences, College of Science, United Arab Emirates University, P. O. Box 15551, Al Ain, United Arab Emirates

ARTICLE INFO

Keywords:
Liver model
Heuristic
Genetic algorithm
Transfer function
Interior point
Simulations

ABSTRACT

In this research, a bio-inspired heuristic computing approach has been developed to solve the nonlinear behavior of the human liver, which is categorized into the liver and blood. The solutions of the human liver model are presented by using the stochastic computation procedure based on the artificial neural network (ANN) along with the optimization of genetic algorithm (GA) and interior-point (IP). A fitness function is designed through the differential form of the nonlinear human liver model and then optimized by using the hybrid competency of GAIP scheme. The correctness and exactness of the proposed approach are observed through the overlapping of the obtained (GAIP) and reference (Adams scheme) solutions, while the calculated absolute error values in good order enhance the worth of the proposed solver. The log-sigmoid transfer function together with ten numbers of neurons is executed to perform the solutions of the human liver nonlinear model. Furthermore, the statistical approaches have been applied in order to observe the reliability of the designed approach for solving the nonlinear human liver model.

1. Introduction

The human liver (HL) is a reddish-brown color organ, which has a position under the diaphragm and the right side of the stomach. Many physiological and metabolic functions, like blood coagulation, digestion, detoxification, nutrient storage, immune system support, and hormone regulation, which are considered essential for good health [1–5]. When the level of blood sugar lows, the liver stores essential nutrients as vitamins and glycogen. Metabolism's waste products, narcotics, and alcohol are some of the hazardous substances, where the liver is responsible for the body's purifying and cleaning out [6,7]. By producing and degrading various forms of the hormones, such as estrogen, insulin, and testosterone, the liver helps to manage the hormonal stability [8]. The process based on HL has several proteins, which are considered crucial for blood coagulation and provide the support to prevent the bleeding from injuries. The liver plays a crucial role in the response of immune in order to produce the monocytes, which is a type of white blood cell that helps to fight against infections [9].

The intricate biological and metabolic process performs better with the help of mathematical models [10]. The metabolism, distribution, excretion, and absorbance pharmacological characteristics along with the consequences of hepatic illnesses present the liver function, which is predicted computationally by exploiting the liver models [11]. The biochemistry form is one of the kinds of mathematical HL, which integrates the spatial arrangement of biochemical events and liver cells [12]. This version of the model

* Corresponding author.
E-mail address: salem.bensaid@uaeu.ac.ae (S. Ben Said).

https://doi.org/10.1016/j.heliyon.2024.e28912
Received 13 May 2023; Received in revised form 23 February 2024; Accepted 26 March 2024
Available online 4 April 2024

depicts the liver's intricate structure, including the placement of sinusoids, bile ducts throughout the organ, and hepatocytes [13]. In addition, the mathematical liver models involve fluid dynamic systems, which simulates the blood's movement and bile by using the pharmacokinetics and liver systems based on the pharmacological properties of the metabolism, distribution, excretion, and absorbance [14]. In the pathological/physiological situations, the modeling of the viral hepatitis and liver injury through drug-induced is presented [15]. There are various kinds of illnesses, which become the disordering reason of liver, like fatty diseases, hepatitis, cirrhosis, and liver cancer [16]. The general form of the HL model is presented below in equation (1) as [17]:

$$\begin{cases} \dfrac{dZ(\theta)}{d\theta} = BW(\theta) - AZ(\theta), Z(0) = i_1, \\ \dfrac{dW(\theta)}{d\theta} = AZ(\theta) - (D+B)W(\theta). \quad W(0) = i_2, \end{cases} \tag{1}$$

where $Z(\theta)$ and $W(\theta)$ indicate the classes of the blood and liver, the initial conditions are i_1 and i_2, while B, A and D are the constants. The mathematical form of the HL model (1) is one of the biological systems, which have already been solved by using the deterministic techniques. However, the stochastic techniques have never been used before to solve the HL model [18]. The current work shows the bio-inspired heuristic computing scheme for the nonlinear HL model, which is categorized into liver and blood. The stochastic artificial neural network (ANN) along with the optimization of genetic algorithm (GA) and interior-point (IP) has been presented to optimize the initial parameters based on the HL. The stochastic paradigms have been implemented in numerous submissions, e.g., differential coronavirus system [19,20], HIV infection [21,22], food chain models [23,24], singular systems [25], singular Poisson-Boltzmann equation [26], nanofluid flow models [27,28], and waste plastic model in ocean [29]. Few prime features of current work are given as:

- The stochastic computing ANN-GAIP solver is applied successfully for the numerical simulations of the HL model.
- The constant, and consistent presentations of the HL system authenticate the exactness of the ANN-GAIP scheme.
- The small and negligible absolute error (AE) values demonstrate the credibility of the ANN-GAIP solver to present the numerical solutions of the HL system.
- The authentication of the approach is prominent by using different statistical performances for forty executions and ten neurons.

The remaining parts of the paper are given as: Sect 2 shows the stochastic structure of the ANN-GAIP solver together with statistical procedures. Sect 3 depicts the solution procedures of the model, while Sect 4 presents the conclusions of this study.

2. Methodology

This section shows the procedure based on the ANN-GAIP scheme for solving the HL model including the error function and the optimization procedures.

2.1. ANN-GAIP procedure

The process of neural network is given in equation (2) as:

$$[\widehat{Z}(\theta), \widehat{W}(\theta)] = \left[\sum_{k=1}^{p} x_{Z,k} L\left(w_{Z,k}\theta + y_{Z,k}\right), \sum_{k=1}^{p} x_{W,k} L\left(w_{W,k}\theta + y_{W,k}\right)\right], \tag{2}$$

$$\left[\frac{d}{d\theta}\widehat{Z}(\theta), \frac{d}{d\theta}\widehat{W}(\theta)\right] = \left[\sum_{k=1}^{p} x_{Z,k} \frac{d}{d\theta} L\left(w_{Z,k}\theta + y_{Z,k}\right), \sum_{k=1}^{p} x_{W,k} \frac{d}{d\theta} L\left(w_{W,k}\theta + y_{W,k}\right)\right],$$

where, L is activation function, $\widehat{Z}$ and $\widehat{W}$ are proposed solutions, p shows the neurons and V is weight vector (unknown), provided as: $\boldsymbol{V} = [\boldsymbol{V}_Z, \boldsymbol{V}_W]$, for $\boldsymbol{V}_W = [\boldsymbol{x}_W, \boldsymbol{\omega}_W, \boldsymbol{y}_W]$, and $\boldsymbol{V}_Z = [\boldsymbol{x}_Z, \boldsymbol{\omega}_Z, \boldsymbol{y}_Z]$, where

$$x_Z = \left[x_{Z,1}, x_{Z,2}, ..., x_{Z,p}\right], x_W = \left[x_{W,1}, x_{W,2}, ..., x_{W,p}\right], w_Z = \left[w_{Z,1}, w_{Z,2}, ..., w_{Z,p}\right],$$
$$w_W = \left[w_{W,1}, w_{W,2}, ..., w_{W,p}\right], y_Z = \left[y_{Z,1}, y_{Z,2}, ..., y_{Z,p}\right], y_W = \left[y_{W,1}, y_{W,2}, ..., y_{W,p}\right],$$

where the activation log-sigmoid function takes the form as $L(\theta) = (1 + \exp(-\theta))^{-1}$, which is provided in equation (3) as:

$$\begin{aligned} [\widehat{Z}(\theta), \widehat{W}(\theta)] &= \left[\sum_{k=1}^{p} \frac{x_{Z,k}}{1 + e^{-\left(w_{Z,k}\theta + y_{Z,k}\right)}}, \sum_{k=1}^{p} \frac{x_{W,k}}{1 + e^{-\left(w_{W,k}\theta + y_{W,k}\right)}}\right], \\ \left[\frac{d}{d\theta}\widehat{Z}(\theta), \frac{d}{d\theta}\widehat{W}(\theta)\right] &= \left[\sum_{k=1}^{p} \frac{w_{Z,k} x_{Z,k} e^{-\left(w_{Z,k}\theta + y_{Z,k}\right)}}{\left(1 + e^{-\left(w_{Z,k}\theta + y_{Z,k}\right)}\right)^2}, \sum_{k=1}^{p} \frac{w_{W,k} x_{W,k} e^{-\left(w_{W,k}\theta + y_{W,k}\right)}}{\left(1 + e^{-\left(w_{W,k}\theta + y_{W,k}\right)}\right)^2}\right]. \end{aligned} \tag{3}$$

A merit function is presented in equation (4) as:

$$\Xi_F = \Xi_{F-1} + \Xi_{F-2} + \Xi_{F-3}, \tag{4}$$

$$\Xi_{F-1} = \frac{1}{N}\sum_{p=1}^{N}\left[\frac{d\widehat{Z}_p}{d\theta} - B\widehat{W}_p + A\widehat{Z}_p\right]^2, \tag{5}$$

$$\Xi_{F-2} = \frac{1}{N}\sum_{p=1}^{N}\left[\frac{d\widehat{Z}_p}{d\theta} - A\widehat{Z}_p + B\widehat{W}_p + D\widehat{W}_p\right]^2, \tag{6}$$

$$\Xi_{F-3} = \frac{1}{2}\left[(\widehat{Z}_0 - i_1)^2 + (\widehat{W}_0 - i_2)^2\right], \tag{7}$$

where equation (5) and equation (6) present the error based fitness functions based on the classes of blood and liver, respectively, while equation (7) is constructed using the initial conditions, and $\widehat{Z}_p = Z(\theta_p), \widehat{W}_p = W(\theta_p), Nh = 1,$ and $\theta_p = hp$.

2.2. GAIP optimization

This section presents the procedure of optimization based on the GAIP scheme for the solutions of the HL model.

GA is one of the global search algorithms that is inspired by using the biological process based on the natural selection. It is generally implemented for solving the optimization models where the optimal solutions are required through the large data set of possible outcomes. GA works through the process of initialization, evaluation, selection, crossover, mutation, evaluation, and elitism. GA is one of the optimizations schemes that is used in vehicle routing [30], diabetes prediction [31], biomarker genes [32], digital twin robots [33], evaluate soil based on the liquefaction [34], liver disease model [35], feature assortment in cancer microarray [36], and cloud service optimization [37].

IP algorithm is an optimization numerical scheme that is applied to solve the linear and quadratic programming models. This approach works through the process of iteration for solving the linear equations by applying the Newton's scheme. This scheme is introduced first time in 1980s and widely applied in various areas, e.g., finance, economics, and engineering. IP scheme has a variety of advantages in the process of optimization and does not need the convex objective function or the linear constraints. IP scheme is implemented in various applications, e.g., model predictive control [38], reactive-power optimization of large-scale power systems [39], dynamic adjustments [40], computationally difficult set covering problems [41], and power system maximum load ability [42]. The hybrid GAIP process is implemented to reduce the sluggishness of the GA global method. The detail of the hybridized GA-IP process is shown in Table 1.

2.3. Performance measures

The statistical forms of the Theil's inequality coefficient (TIC), variance account for (VAF), and semi-interquartile range (SIR) are mathematically defined in equations (8)–(10) as:

$$\begin{cases} \mathrm{S} - \mathrm{I} - \mathrm{R} = -0.5(Q_1 - Q_3), \\ Q_1 \text{ and } Q_3 = 1^{\text{st}} \text{ and } 3^{\text{rd}} \text{ quartile}, \end{cases} \tag{8}$$

Table 1
Optimization of the scheme for solving the HL model.

GA starts
Inputs: For similar networks, the chromosomes: $\boldsymbol{W} = [\boldsymbol{x}, \boldsymbol{w}, \boldsymbol{y}]$
Population: Chromosomes are $V_W = [\boldsymbol{x}_W, \boldsymbol{\omega}_W, \boldsymbol{y}_W]$, and $V_Z = [\boldsymbol{x}_Z, \boldsymbol{\omega}_Z, \boldsymbol{y}_Z]$.
Output: Optimal global weights: $\boldsymbol{W}_{\mathbf{GA}}$
Initiates: The chromosomes assortment is regulated as $\boldsymbol{W}_{\mathbf{GA}}$.
Fitness Evaluation: Set the Fitness (Ξ_F) for the population ($\boldsymbol{P}$).
- **Stopping specifications**: [Ξ_F = TolFun = TolCon = 10^{-19}], [PopSize = 270], [Generations = 70], and [StallLimit = 200].

Then Store
Ranking: Optimal WGA in the population.
Storage: Time, $\boldsymbol{W}_{\mathbf{GA}}$, generation, count of function, Ξ_F for GA measures
GA ends
IP Starts
Inputs: $\boldsymbol{W}_{\mathbf{GA}}$
Output: Best GAIP weights are $\boldsymbol{W}_{\mathbf{GAIP}}$
Adjust: $\boldsymbol{W}_{\mathbf{GAIP}}$ values, assignments, and iterations.
Termination: [MaxFunEvals = 280000], [Generations = 750], & [TolFun = Ξ_F = TolX = 10^{-21}].
FIT calculation: $\boldsymbol{W}_{\mathbf{GAIP}}$ and Ξ_F for Eqs 4–7.
Modifications: Normalize 'fmincon' for IP scheme, Ξ_F to update '$\boldsymbol{W}$'.
Accumulate: Best $\boldsymbol{W}_{\mathbf{GAIP}}$ values, Ξ_F, time, & func counts.
IP End

$$\begin{cases} [\mathrm{VAF}_Z, \mathrm{VAF}_W] = \left[\left(1 - \dfrac{\mathrm{var}(Z_p - \widehat{Z}_p)}{\mathrm{var}(Z_p)}\right) * 100, \left(1 - \dfrac{\mathrm{var}(W_p - \widehat{W}_p)}{\mathrm{var}(W_p)}\right) * 100,\right] \\ [\mathrm{EVAF}_x, \mathrm{EVAF}_y] = [|100 - \mathrm{VAF}_Z|, |100 - \mathrm{VAF}_W|], \end{cases} \tag{9}$$

$$[\mathrm{TIC}_Z, \mathrm{TIC}_W] = \left[\frac{\sqrt{\frac{1}{n}\sum_{p=1}^{n}(Z_p - \widehat{Z}_p)^2}}{\left(\sqrt{\frac{1}{n}\sum_{p=1}^{n} Z_p^2} + \sqrt{\frac{1}{n}\sum_{p=1}^{n} \widehat{Z}_p^2}\right)}, \frac{\sqrt{\frac{1}{n}\sum_{p=1}^{n}(W_p - \widehat{W}_p)^2}}{\left(\sqrt{\frac{1}{n}\sum_{p=1}^{n} W_p^2} + \sqrt{\frac{1}{n}\sum_{p=1}^{n} \widehat{W}_p^2}\right)}\right], \tag{10}$$

3. Results of the HL model

This section presents the numerical results of the HL model (1) by applying the stochastic procedures based on the ANN-GAIP scheme. The overlapping of the results, weights, performance representations, and the graphs of AE are also illustrated in this section. The mathematical form by taking the suitable values is given in equation (11) as:

$$\begin{cases} \dfrac{dZ(\theta)}{d\theta} = 0.2W(\theta) - 0.1Z(\theta), Z(0) = 1, \\ \dfrac{dW(\theta)}{d\theta} = 0.1Z(\theta) - 0.5W(\theta), W(0) = 1. \end{cases} \tag{11}$$

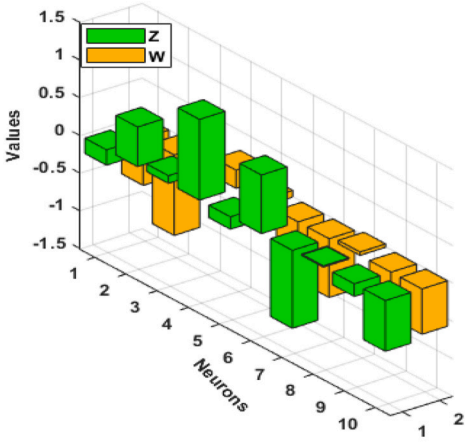

(a): Optimal weights: $Z(\theta)$

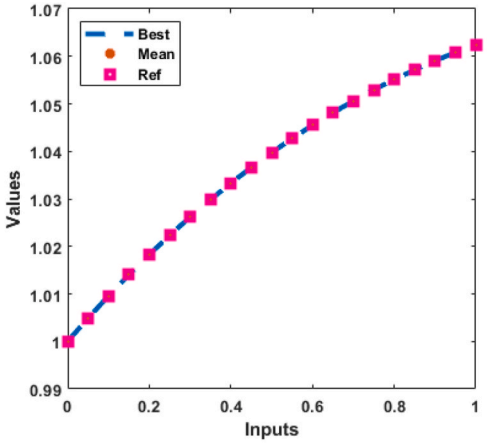

(c) Comparison: $Z(\theta)$

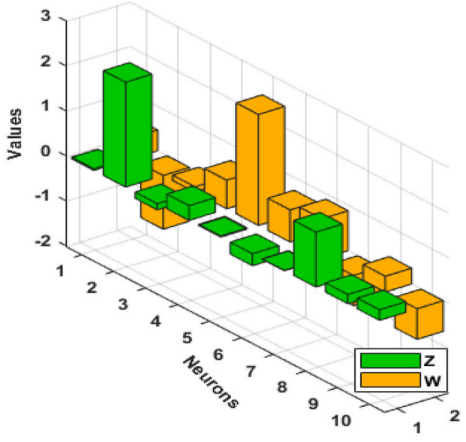

(b): Optimal weights: $W(\theta)$

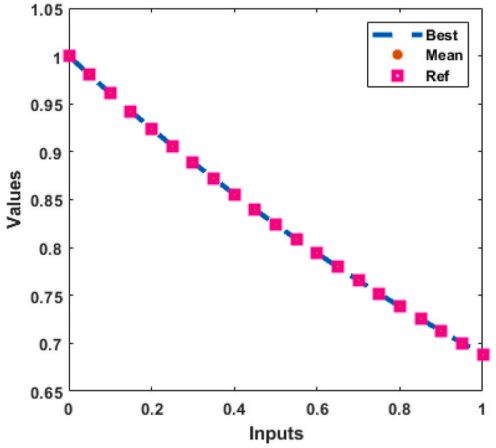

(d) Comparison: $W(\theta)$

Fig. 1. Optimal vectors and comparisons for the HL model.

A merit function using Eq. (4) is given in equation (12) as:

$$\Xi_F = \frac{1}{N}\sum_{p=1}^{N}\left(\left[\frac{d\widehat{Z}_p}{d\theta} - 0.2\widehat{W}_p + 0.1\widehat{Z}_p\right]^2 + \left[\frac{d\widehat{Z}_p}{d\theta} - 0.1\widehat{Z}_p + 0.5\widehat{W}_p\right]^2\right) + \frac{1}{2}\left[(\widehat{Z}_0 - 1)^2 + (\widehat{W}_0 - 1)^2\right]. \tag{12}$$

The optimization of an error function using the ANN-GAIP is performed for solving the HL model (1) in order to accomplish the neural network parameters by taking 10 neurons. The optimal performances of the weight vectors for solving the HL model are provided in equations (13) and (14) as:

$$\begin{aligned}\widehat{Z}(\theta) = {} & \frac{-0.2034}{1+e^{-(-0.628\theta+0.2245)}} + \frac{0.5252}{1+e^{-(-1.069\theta-0.3096)}} + \frac{0.1014}{1+e^{-(-0.099\theta+0.2601)}} + \frac{1.0709}{1+e^{-(0.2423\theta+1.4044)}} - \frac{0.1645}{1+e^{-(0.0885\theta-1.5293)}} \\ & + \frac{0.7774}{1+e^{-(-0.6937\theta+1.2594)}} + \frac{0.0164}{1+e^{-(0.0450\theta+0.1560)}} - \frac{1.0344}{1+e^{-(-0.780\theta-1.121)}} - \frac{0.1677}{1+e^{-(0.4659\theta+0.6281)}} - \frac{0.6735}{1+e^{-(-0.6025\theta-0.5414)}},\end{aligned} \tag{13}$$

$$\begin{aligned}\widehat{W}(\theta) = {} & \frac{0.0368}{1+e^{-(0.4624\theta-0.0380)}} + \frac{2.3314}{1+e^{-(-1.1966\theta-2.4553)}} - \frac{0.1351}{1+e^{-(0.1185\theta-1.8381)}} + \frac{0.3279}{1+e^{-(0.6362\theta+0.7386)}} + \frac{0.0236}{1+e^{-(2.4678\theta+1.7083)}} \\ & - \frac{0.2669}{1+e^{-(0.7155\theta+0.2690)}} - \frac{0.0101}{1+e^{-(0.8883\theta-0.7693)}} + \frac{1.2213}{1+e^{-(-0.6767\theta-0.5614)}} + \frac{0.2062}{1+e^{-(0.3516\theta+0.1141)}} + \frac{0.2357}{1+e^{-(-0.6816\theta+1.0708)}}.\end{aligned} \tag{14}$$

The optimal weights and result's comparisons for both dynamics of HL model are shown in Fig. 1. Ten numbers of neurons and the weight vectors are shown in Fig. 1(a to b) based on Eqs. (13) and (14). Fig. 1(c to d) illustrates the accuracy of the approach for solving the HL model using the best, mean, and even worst solutions. Fig. 2 (a and b) shows the mean/best AE performances for solving the HL model. The optimal performances are found as 10^{-06}-10^{-08} and 10^{-07}-10^{-09}, while the AE mean measures are shown as 10^{-06}-10^{-07} for the dynamics $Z(\theta)$ and $W(\theta)$. These small measures based on the AE improve the precision of the designed ANN-GAIP scheme for the HL model. The TIC performances for solving the HL model are performed in Fig. 3(a), while the histogram based on the TIC are presented in Fig. 3(b) and (c). These values are measured around 10^{-09} to 10^{-11} for each class of the HL model. Fig. 4 (a) displays the EVAF results for the stochastic technique that has been applied to solve the HL model, which are stated as 10^{-08} to 10^{-12} for both classes of the nonlinear system, while the histogram based on the EVAF are illustrated in Figs. 4(b) and 3(c). These optimal performances of the statistical operators develop the consistency of the approach.

Tables 2 and 3 shows the statistical operators base on the minimum (optimal results), standard deviation (SD), maximum (worst outputs), mean, median, and S–I-R. The optimal results are accomplished as 10^{-08}-10^{-11} and 10^{-07}-10^{-10} for $Z(\theta)$ and $W(\theta)$. The values of the worst outputs also presented as 10^{-05}-10^{-06} for $Z(\theta)$ and $W(\theta)$. The other statistical operators based on the mean, S–I-R and median values are presented as 10^{-06}-10^{-07} for both classes of the HL model. It is confirmed that the designed solver accurately performs the nonlinear dynamics of HL based on the statistical interpretations.

4. Conclusions

The current investigations are related to perform a bio-inspired heuristic computing approach, which has been developed to solve the nonlinear behavior of the human liver. The mathematical form of the nonlinear human liver model is presented into two categories, liver, and blood. Few comprehensive conclusions of this study are presented as.

- The stochastic performances using the procedures of ANN-GAIP solver have been performed successfully to solve the nonlinear dynamics of the human liver.

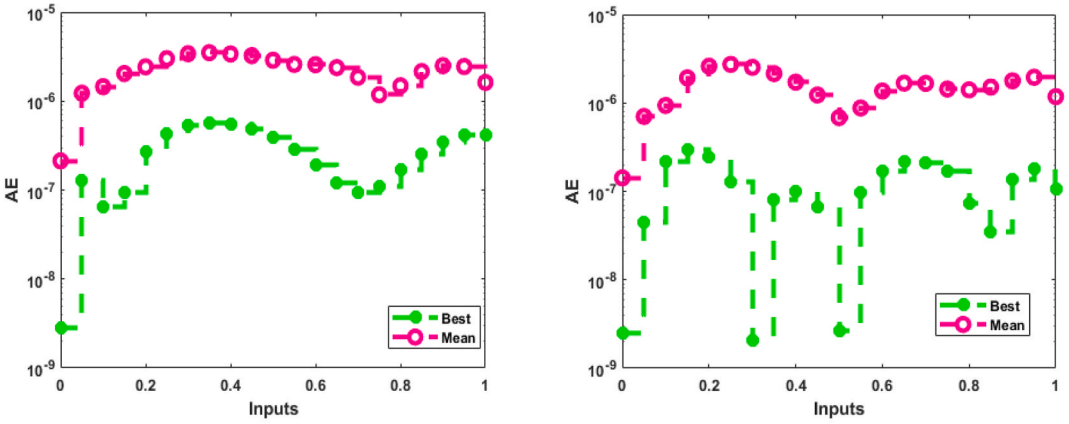

(a): AE: $Z(\theta)$ (b) AE: $Z(\theta)$

Fig. 2. Best/mean values of the AE for the HL model.

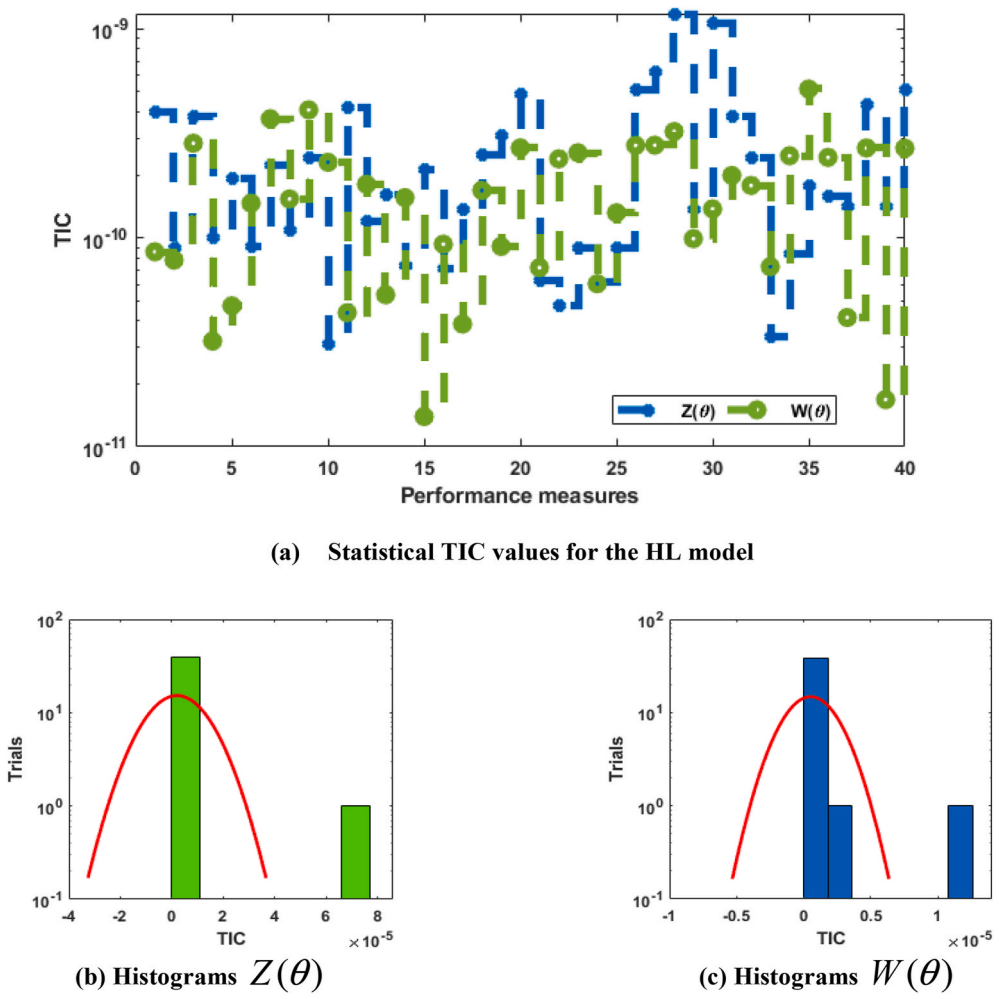

Fig. 3. Statistical TIC values and histogram to solve the HL model.

- A design of fitness function is performed through the differential human liver model and then optimize by using the hybrid competency of the GAIP scheme.
- The log-sigmoid transfer function, ten numbers of neurons, and forty numbers of runs have been executed to solve the human liver nonlinear model.
- The exactly overlapping of the obtained and reference results provide the exactness of the approach.
- The competence of the scheme is examined through the AE values, which has been performed around 10^{-06} to 10^{-06} for both categories of the model.
- The statistical approaches based on the TIC and EVAF operators provide the reliability of the approach by using 40 trials.
- The operator based on Min, Max, Med, Mean, S–I-R and SD are also provided in small measures, which shows the consistency of the designed scheme.

In future, the nonlinear forms of the models will be numerically discussed by using different stochastic approaches.

CRediT authorship contribution statement

Zulqurnain Sabir: Software, Resources, Methodology, Investigation, Formal analysis. **Salem Ben Said:** Writing – review & editing, Supervision. **Qasem Al-Mdallal:** Writing – review & editing, Visualization, Validation, Supervision.

Declaration of competing interest

There is not any potential competing or non-financial declaration of competing interests on behalf of all authors of the manuscript.

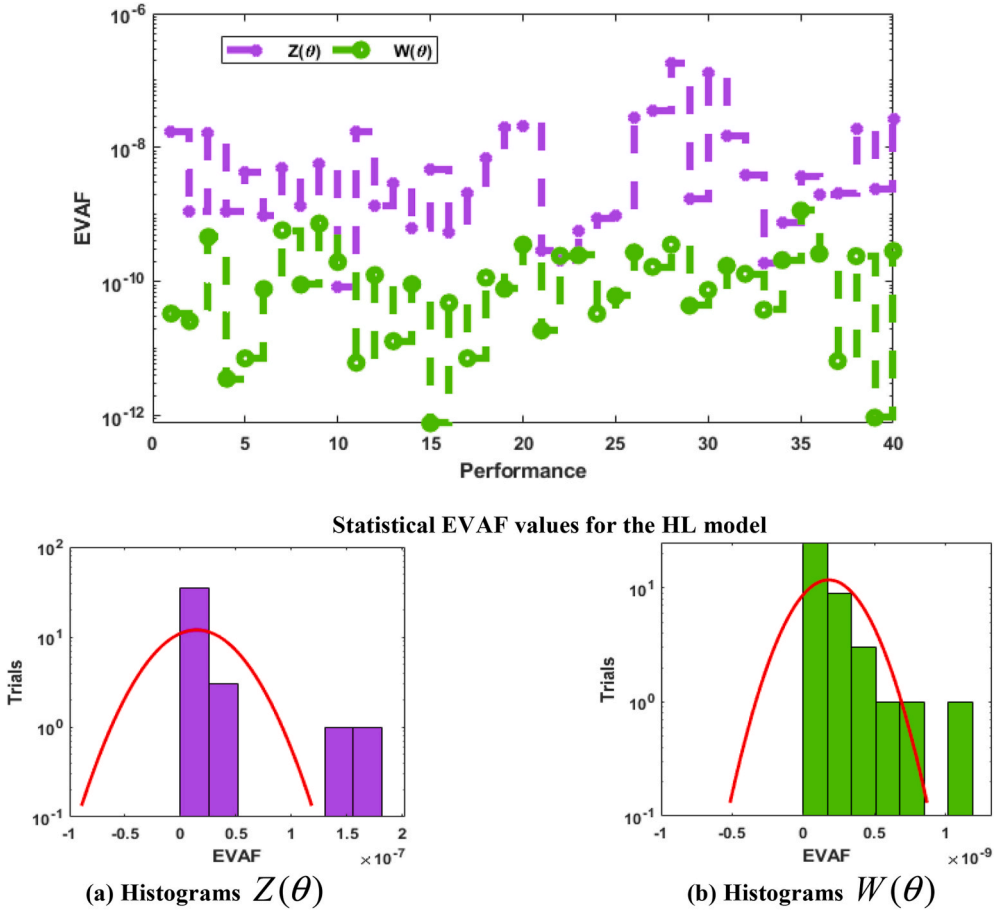

Fig. 4. Statistical EVAF values and histogram to solve the HL model.

Table 2
Statistical operator values for the HL model-based dynamics $Z(\theta)$.

θ	$Z(\theta)$					
	Min	Max	Med	Mean	S–I-R	SD
0	3.22773E-11	2.67096E-06	2.67106E-09	2.13170E-07	3.62568E-08	5.21191E-07
0.05	1.03822E-08	5.72627E-06	5.19782E-07	1.22811E-06	7.13805E-07	1.62448E-06
0.1	7.85048E-09	6.67184E-06	6.28292E-07	1.45156E-06	6.41601E-07	1.92848E-06
0.15	4.29220E-08	7.16898E-06	1.75342E-06	2.04106E-06	1.04394E-06	1.52302E-06
0.2	4.97287E-08	6.85302E-06	1.97972E-06	2.42927E-06	8.38460E-07	1.91257E-06
0.25	8.39352E-08	9.27758E-06	2.05475E-06	2.99957E-06	1.23748E-06	2.62265E-06
0.3	4.52611E-08	1.46635E-05	1.96107E-06	3.41046E-06	1.66108E-06	3.46039E-06
0.35	3.05189E-08	1.92209E-05	1.77443E-06	3.50581E-06	1.64519E-06	4.26012E-06
0.4	5.04060E-08	2.21939E-05	1.33424E-06	3.38627E-06	1.84181E-06	4.83759E-06
0.45	2.34017E-08	2.33833E-05	1.42922E-06	3.24897E-06	1.48376E-06	5.06518E-06
0.5	2.54868E-08	2.27949E-05	8.94838E-07	2.88249E-06	8.45574E-07	5.10018E-06
0.55	1.99851E-08	2.06181E-05	5.59425E-07	2.58317E-06	8.54350E-07	4.76605E-06
0.6	5.37955E-09	1.71659E-05	8.79306E-07	2.56590E-06	1.00887E-06	3.93993E-06
0.65	1.21082E-07	1.28750E-05	1.27315E-06	2.38321E-06	1.21462E-06	2.87751E-06
0.7	7.01617E-08	8.24539E-06	1.37606E-06	1.85460E-06	9.52101E-07	1.86529E-06
0.75	3.87237E-08	5.06061E-06	7.42079E-07	1.17914E-06	5.93018E-07	1.28326E-06
0.8	1.70248E-07	4.70051E-06	1.12712E-06	1.48844E-06	8.28143E-07	1.16063E-06
0.85	1.87374E-08	7.76407E-06	1.42023E-06	2.15029E-06	1.01576E-06	1.80750E-06
0.9	1.65049E-08	9.42596E-06	1.50256E-06	2.50368E-06	1.51462E-06	2.50362E-06
0.95	2.32475E-08	8.67747E-06	1.49946E-06	2.45138E-06	1.62996E-06	2.46156E-06
1	3.51364E-10	5.91568E-06	8.55578E-07	1.62147E-06	9.45705E-07	1.73399E-06

Table 3
Statistical operator values for the HL model-based dynamics $W(\theta)$.

θ	$W(\theta)$					
	Min	Max	Med	Mean	S–I-R	SD
0	1.38467E-10	2.13707E-06	5.93706E-09	2.13170E-07	2.12080E-08	3.83096E-07
0.05	3.74092E-08	3.35835E-06	3.77610E-07	1.22811E-06	3.77076E-07	8.34601E-07
0.1	2.51972E-08	5.36001E-06	4.48420E-07	1.45156E-06	5.78655E-07	1.14687E-06
0.15	5.03213E-08	6.79411E-06	1.47337E-06	2.04106E-06	1.07115E-06	1.52009E-06
0.2	7.52814E-08	7.85484E-06	2.29706E-06	2.42927E-06	1.43161E-06	1.84356E-06
0.25	7.22031E-08	1.01621E-05	2.57840E-06	2.99957E-06	1.45151E-06	2.17024E-06
0.3	2.05938E-09	1.06600E-05	1.71600E-06	3.41046E-06	1.35076E-06	2.27196E-06
0.35	6.17825E-08	9.46966E-06	1.40423E-06	3.50581E-06	1.24600E-06	2.09482E-06
0.4	1.01446E-07	7.02502E-06	1.27291E-06	3.38627E-06	9.55864E-07	1.64478E-06
0.45	6.59223E-08	4.95089E-06	9.23818E-07	3.24897E-06	7.78127E-07	1.11829E-06
0.5	2.68648E-09	3.75556E-06	3.14251E-07	2.88249E-06	2.94169E-07	9.05448E-07
0.55	2.02002E-08	3.55599E-06	6.94076E-07	2.58317E-06	5.29199E-07	8.86700E-07
0.6	4.40008E-08	4.56264E-06	1.29950E-06	2.56590E-06	7.98119E-07	1.13106E-06
0.65	1.71345E-07	6.36552E-06	1.38576E-06	2.38321E-06	9.80623E-07	1.43498E-06
0.7	1.63372E-07	7.01747E-06	1.04963E-06	1.85460E-06	7.35626E-07	1.65544E-06
0.75	7.41047E-08	6.34871E-06	7.30443E-07	1.17914E-06	5.62936E-07	1.63140E-06
0.8	2.52505E-08	4.58459E-06	8.88002E-07	1.48844E-06	8.01158E-07	1.25973E-06
0.85	2.94338E-08	4.63580E-06	1.29656E-06	2.15029E-06	8.76862E-07	1.26492E-06
0.9	5.47720E-08	6.57784E-06	1.00035E-06	2.50368E-06	1.15850E-06	1.68308E-06
0.95	4.82259E-08	6.89769E-06	1.43046E-06	2.45138E-06	1.15787E-06	1.72695E-06
1	6.98446E-08	4.62217E-06	7.78969E-07	1.62147E-06	6.41585E-07	1.10981E-06

Acknowledgement

The authors are thankful to United Arab Emirates University for the financial support through the UPAR grant number 12S121.

References

[1] Z.Y. Dong, B.J. Xiang, M. Jiang, M.J. Sun, C. Dai, The prevalence of gastrointestinal symptoms, abnormal liver function, digestive system disease and liver disease in COVID-19 infection: a systematic review and meta-analysis, J. Clin. Gastroenterol. 55 (1) (2021) 67.
[2] Y. Wang, T. Nakajima, F.J. Gonzalez, N. Tanaka, PPARs as metabolic regulators in the liver: lessons from liver-specific PPAR-null mice, Int. J. Mol. Sci. 21 (6) (2020) 2061.
[3] P. Kur, A. Kolasa-Wołosiuk, K. Misiakiewicz-Has, B. Wiszniewska, Sex hormone-dependent physiology and diseases of liver, Int. J. Environ. Res. Publ. Health 17 (8) (2020) 2620.
[4] Uzung Yoon, Justyna Bartoszko, Dmitri Bezinover, Gianni Biancofiore, Katherine T. Forkin, Suehana Rahman, Michael Spiro, et al., Intraoperative transfusion management, antifibrinolytic therapy, coagulation monitoring and the impact on short-term outcomes after liver transplantation—a systematic review of the literature and expert panel recommendations, Clin. Transplant. 36 (10) (2022) e14637.
[5] F. Li, Y. Qiu, F. Xia, H. Sun, H. Liao, A. Xie, J. Lee, P. Lin, M. Wei, Y. Shao, B. Yang, Dual detoxification and inflammatory regulation by ceria nanozymes for drug-induced liver injury therapy, Nano Today 35 (2020) 100925.
[6] N. Topić Popović, L. Čižmek, S. Babić, I. Strunjak-Perović, R. Čož-Rakovac, Fish liver damage related to the wastewater treatment plant effluents, Environ. Sci. Pollut. Control Ser. (2023) 1–30.
[7] X. Capó, M. Morató, C. Alomar, B. Rios-Fuster, M. Valls, M. Compa, S. Deudero, A biomarker approach as responses of bioindicator commercial fish species to microplastic ingestion: assessing tissue and biochemical relationships, Biology 11 (11) (2022) 1634.
[8] R. Palma, A. Pronio, M. Romeo, F. Scognamiglio, L. Ventriglia, V.M. Ormando, A. Lamazza, S. Pontone, A. Federico, M. Dallio, The role of insulin resistance in fueling NAFLD pathogenesis: from molecular mechanisms to clinical implications, J. Clin. Med. 11 (13) (2022) 3649.
[9] D.G. Ko, J.W. Park, J.H. Kim, J.H. Jung, H.S. Kim, K.T. Suk, M.K. Jang, S.H. Park, M.S. Lee, D.J. Kim, S.E. Kim, Platelet-to-White blood cell ratio: a feasible biomarker for pyogenic liver abscess, Diagnostics 12 (10) (2022) 2556.
[10] F.A. Romero, C.T. Jones, Y. Xu, M. Fenaux, R.L. Halcomb, The race to bash NASH: emerging targets and drug development in a complex liver disease, J. Med. Chem. 63 (10) (2020) 5031–5073.
[11] A. Zhang, K. Meng, Y. Liu, Y. Pan, W. Qu, D. Chen, S. Xie, Absorption, distribution, metabolism, and excretion of nanocarriers in vivo and their influences, Adv. Colloid Interface Sci. 284 (2020) 102261.
[12] T.K. Fakhry, R. Mhaskar, T. Schwitalla, E. Muradova, J.P. Gonzalvo, M.M. Murr, Bariatric surgery improves nonalcoholic fatty liver disease: a contemporary systematic review and meta-analysis, Surg. Obes. Relat. Dis. 15 (3) (2019) 502–511.
[13] F. Chen, R.J. Jimenez, K. Sharma, H.Y. Luu, B.Y. Hsu, A. Ravindranathan, B.A. Stohr, H. Willenbring, Broad distribution of hepatocyte proliferation in liver homeostasis and regeneration, Cell Stem Cell 26 (1) (2020) 27–33.
[14] A.J. Ribeiro, X. Yang, V. Patel, R. Madabushi, D.G. Strauss, Liver microphysiological systems for predicting and evaluating drug effects, Clin. Pharmacol. Therapeut. 106 (1) (2019) 139–147.
[15] C.C. Wang, P.N. Cheng, J.H. Kao, Systematic review: chronic viral hepatitis and metabolic derangement, Aliment. Pharmacol. Ther. 51 (2) (2020) 216–230.
[16] T. Kanda, T. Goto, Y. Hirotsu, M. Moriyama, M. Omata, Molecular mechanisms driving progression of liver cirrhosis towards hepatocellular carcinoma in chronic hepatitis B and C infections: a review, Int. J. Mol. Sci. 20 (6) (2019) 1358.
[17] M. Azeem, M. Farman, M. Abukhaled, K.S. Nisar, A. Akgul, Epidemiological analysis of the human liver model with a fractional operator, Fractals 31 (04) (2023) 2340047.
[18] T. Botmart, Z. Sabir, M.A.Z. Raja, R. Sadat, M.R. Ali, Stochastic procedures to solve the nonlinear mass and heat transfer model of Williamson nanofluid past over a stretching sheet, Ann. Nucl. Energy 181 (2023) 109564.
[19] Z. Sabir, M. Umar, M.A.Z. Raja, D. Baleanu, Applications of Gudermannian neural network for solving the SITR fractal system, Fractals 29 (8) (2021) 2150250.
[20] Z. Sabir, A.S. Alnahdi, M.B. Jeelani, M.A. Abdelkawy, M.A.Z. Raja, D. Baleanu, M.M. Hussain, Numerical computational heuristic through morlet wavelet neural network for solving the dynamics of nonlinear sitr covid-19, Cmes-Computer Modeling in Engineering & Sciences (2022) 763–785.
[21] M. Umar, Z. Sabir, M.A.Z. Raja, H.M. Baskonus, S.W. Yao, E. Ilhan, A novel study of Morlet neural networks to solve the nonlinear HIV infection system of latently infected cells, Results Phys. 25 (2021) 104235.

[22] Y.G. Sanchez, M. Umar, Z. Sabir, J.L. Guirao, M.A.Z. Raja, Solving a class of biological HIV infection model of latently infected cells using heuristic approach, Discrete. Contin. Dyn. Syst. S 14 (2018).
[23] Z. Sabir, Stochastic numerical investigations for nonlinear three-species food chain system, Int. J. Biomath. (IJB) 15 (4) (2022) 2250005.
[24] Z. Sabir, M.R. Ali, R. Sadat, Gudermannian neural networks using the optimization procedures of genetic algorithm and active set approach for the three-species food chain nonlinear model, J. Ambient Intell. Hum. Comput. (2022) 1–10.
[25] Z. Sabir, F. Amin, D. Pohl, J.L. Guirao, Intelligence computing approach for solving second order system of Emden–Fowler model, J. Intell. Fuzzy Syst. 38 (6) (2020) 7391–7406.
[26] N. Yousaf, R. Nasir, S. Rafique, A. Zameer, N.M. Mirza, PCGA: polynomial collocation genetic algorithm for singular Poisson-Boltzmann equation arising in thermal explosions, Heliyon 9 (4) (2023) 12345.
[27] M. Shoaib, R. Tabassum, K.S. Nisar, M.A.Z. Raja, N. Fatima, N. Al-Harbi, A.H. Abdel-Aty, A design of neuro-computational approach for double-diffusive natural convection nanofluid flow, Heliyon 9 (3) (2023) 12345.
[28] M. Shoaib, F.A. Shah, K.S. Nisar, M.A.Z. Raja, E. ul Haq, A.Z. Abbasi, Q.M.U. Hassan, N. Al-Harbi, A.H. Abdel-Aty, Variational iteration method along with intelligent computing system for the radiated flow of electrically conductive viscous fluid through porous medium, Heliyon 9 (3) (2023) 12345.
[29] M. AL Nuwairan, Z. Sabir, M. Asif Zahoor Raja, A. Aldhafeeri, An advance artificial neural network scheme to examine the waste plastic management in the ocean, AIP Adv. 12 (4) (2022) 045211.
[30] B.M. Baker, M. Ayechew, A genetic algorithm for the vehicle routing problem, Comput. Oper. Res. 30 (5) (2003) 787–800.
[31] S. Bhat, M.G. Jagadeeshaprasad, V. Venkatasubramani, M.J. Kulkarni, Abundance matters: role of albumin in diabetes, a proteomics perspective, Expet Rev. Proteonomics 14 (8) (2017) 677–689.
[32] M. Sathya, M. Jeyaselvi, S. Joshi, E. Pandey, P.K. Pareek, S.S. Jamal, V. Kumar, H.K. Atiglah, Cancer categorization using genetic algorithm to identify biomarker genes, Journal of Healthcare Engineering 2022 (2022).
[33] X. Liu, D. Jiang, B. Tao, G. Jiang, Y. Sun, J. Kong, X. Tong, G. Zhao, B. Chen, Genetic algorithm-based trajectory optimization for digital twin robots, Front. Bioeng. Biotechnol. 9 (2022) 1433.
[34] J. Zhou, S. Huang, M. Wang, Y. Qiu, Performance evaluation of hybrid GA–SVM and GWO–SVM models to predict earthquake-induced liquefaction potential of soil: a multi-dataset investigation, Eng. Comput. (2021) 1–19.
[35] G.A. Rao, E.C. Larkin, Nutritional factors required for alcoholic liver disease in rats, J. Nutr. 127 (5) (1997) 896S–898S.
[36] S. Sayed, M. Nassef, A. Badr, I. Farag, A nested genetic algorithm for feature selection in high-dimensional cancer microarray datasets, Expert Syst. Appl. 121 (2019) 233–243.
[37] Y. Yang, B. Yang, S. Wang, F. Liu, Y. Wang, X. Shu, A dynamic ant-colony genetic algorithm for cloud service composition optimization, Int. J. Adv. Des. Manuf. Technol. 102 (2019) 355–368.
[38] Y.C. Wu, A.S. Debs, R.E. Marsten, A direct nonlinear predictor-corrector primal-dual interior point algorithm for optimal power flows, IEEE Trans. Power Syst. 9 (2) (1994) 876–883.
[39] M. Liu, S.K. Tso, Y. Cheng, An extended nonlinear primal-dual interior-point algorithm for reactive-power optimization of large-scale power systems with discrete control variables, IEEE Trans. Power Syst. 17 (4) (2002) 982–991.
[40] X. Yan, V.H. Quintana, Improving an interior-point-based OPF by dynamic adjustments of step sizes and tolerances, IEEE Trans. Power Syst. 14 (2) (1999) 709–717.
[41] N. Karmarkar, M.G. Resende, K.G. Ramakrishnan, An interior point algorithm to solve computationally difficult set covering problems, Math. Program. 52 (1991) 597–618.
[42] Youjie Dai, James D. McCalley, Vijay Vittal, Simplification, expansion and enhancement of direct interior point algorithm for power system maximum loadability, in: Proceedings of the 21st International Conference on Power Industry Computer Applications. Connecting Utilities. PICA 99. To the Millennium and beyond (Cat. No. 99CH36351), IEEE, 1999, pp. 193–201.